CHAPTER 14

THE DIFFRACTIVE MULTIFOCAL FOCUSING EFFECT

John T. Foley, Renat R. Letfullin, and Henk F. Arnoldus

14.1 Introduction

It is well known that when a monochromatic plane wave of intensity I_o is normally incident upon a circular aperture, the intensity at on-axis observation points behind the aperture oscillates between the values $4I_o$ and zero as the distance from the aperture is increased. The reason for this is that the various Fresnel zones in the aperture contribute either constructively or destructively to the amplitude of the field at the observation point in question, causing the amplitude to oscillate between zero and twice the incident field value. For an incident wavelength λ, aperture radius a, and aperture-plane to observation-plane distance z, the number of zones that contribute is given by the Fresnel number, $N = a^2/\lambda z$. The maxima and minima occur at observation points where the Fresnel number is an odd or even integer, respectively.

What is commonly not recognized is the fact that in the region near the z-axis, as z is increased, the light is repeatedly focusing and defocusing, over and over again due to diffraction. The focal points occur at positions where the Fresnel number is an odd integer. This was pointed out in a series of papers by Lit and coworkers [1–3] and most recently by Letfullin and George [4], who referred to this phenomenon as the diffractive multifocal focusing of radiation (DMFR) effect.

Letfullin and George proposed to use a system of two circular apertures for which the on-axis intensity of an incident monochromatic plane wave would increase dramatically due to the DMFR effect. In their system the second aperture was located where the Fresnel number of the first aperture was unity. They analyzed this system theoretically, and showed that the on-axis intensity behind the second aperture oscillates between maximum values of the order of 10 times that of the incident wave and minimum values that are very small, but not zero. These

predictions were verified experimentally [5,6] and extended theoretically to incident fields with a Gaussian amplitude distribution [7]. In Refs. [4–7] the phase of the field was not investigated.

In this chapter we investigate the intensity and phase of the diffracted field behind a circular aperture when a monochromatic plane wave is incident upon it, and when a monochromatic Gaussian beam is incident upon it. We also investigate the intensity and phase of the diffracted field behind a system of two circular apertures for the same two incident fields. In each case we substantiate the focusing, defocusing and refocusing interpretation mentioned above, and investigate the intensity at the focal points.

In Sect. 14.2.1 we show that when a plane wave is incident upon a single circular aperture, in the neighborhood of a focal point (where the Fresnel number is odd) the phase of the wave approaching the focal point is that of a converging wave, the phase front in the focal plane is planar, and the phase of the wave exiting the focal point is that of a diverging wave. We also show that the wave becomes more and more divergent as the distance from the focal point is increased, until a position is reached where the Fresnel number is even. At such a point the intensity of the wave is zero, and the phase of the wave is undefined, i.e., singular. We show that as the on-axis observation point moves away from the aperture and passes through a singular point, the nature of the wave in the neighborhood of the axis changes from that of a diverging wave to that of a converging wave, i.e., the wave refocuses. In Sect. 14.2.2 we show that when the incident field is a Gaussian beam, the phase behaves similarly, and the intensities at the focal points decrease as the ratio of the radius of the aperture to the spot size of the incident beam is increased.

In Sect. 14.3.1 we use the results of Sect. 14.2 to investigate the intensity and the phase of the field after the second aperture in a system of two circular apertures when a plane wave is incident. In this case the ratio of the radii of the two apertures is a key parameter, and we discuss the effect of varying this ratio. In Sect. 14.3.2, we do the same for a Gaussian beam incident upon a two aperture system.

We use scalar wave theory throughout this paper. Unlike in Refs. [4] and [7], where the monochromatic wave equation (the Helmholtz equation) was integrated numerically, we use the Fresnel approximation and the paraxial approximation in our calculations.

14.2 Fresnel Diffraction by a Circular Aperture

14.2.1 Incident plane wave

14.2.1.1 Basic equations

Consider a monochromatic plane wave of amplitude U_o and angular frequency ω, propagating in the positive z-direction, and normally incident upon an opaque screen in the plane $z = 0$, containing an aperture of radius a. The aperture is centered about the origin. Let $P' = (x', y', 0)$ be a point inside the aperture, and let $P = (x, y, z)$ be a point in an observation plane $z =$ constant > 0 (see Fig. 1). In cylindrical polar coordinates we have $P' = (\rho', \theta', 0)$ and $P = (\rho, \theta, z)$. We assume a time dependence of $\exp(-i\omega t)$ for the field. The complex amplitude, $U^{(i)}(\rho, \theta, z)$, of the incident field is given by

$$U^{(i)}(\rho, \theta, z) = U_o e^{ikz}, \tag{1}$$

where U_o is a positive constant and $k = \omega/c$ is the wave number of the light.

We make the following assumptions. First, that the wavelength λ is much smaller than the distance z from the aperture plane to the observation plane. Second, that the Fresnel number of the observation plane is small, and that the trans-

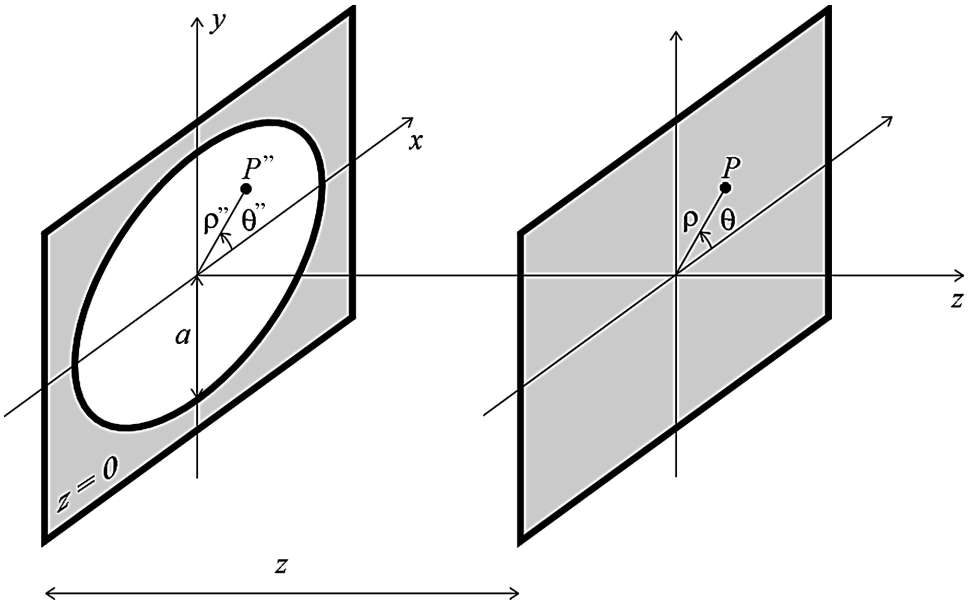

Figure 1 Geometry for the diffraction of a plane wave from a circular aperture with radius a. Point $P' = (\rho', \theta', 0)$ is a point inside the aperture and $P = (\rho, \theta, z)$ is a point in the observation plane $z =$ constant.

verse distance ρ is less than the aperture radius a and much less than the distance z. In this case the paraxial form of the Fresnel approximation to the Rayleigh-Sommerfeld diffraction formula [8] is appropriate for describing the field. The complex amplitude, $U(\rho, \theta, z)$, of the diffracted field can then be written as

$$U(\rho,\theta,z) = \frac{k}{2\pi i z} U_o e^{ikz} e^{ik\rho^2/2z} \times \int_0^a \int_0^{2\pi} U^{(i)}(\rho',\theta',0) e^{ik\rho'^2/2z} e^{-ik\rho\rho'\cos(\theta-\theta')/z} \rho' d\rho' d\theta'. \tag{2}$$

Equation (2) is equivalent to the formula used by Lommel [9] for the case in which the incident field is a diverging spherical wave.

Let us now simplify this equation. Upon substituting the value of $U(\rho', \theta', 0)$ from Eq. (1) into this equation and performing the angular integration, we find that the complex amplitude of the field is independent of the angle θ and is given by the expression

$$U(\rho,z) = \frac{k}{iz} U_o e^{ikz} e^{ik\rho^2/2z} \int_0^a e^{ik\rho'^2/2z} J_0(k\rho\rho'/z)\rho' d\rho', \tag{3}$$

where $J_0(x)$ is the zero-order Bessel function of the first kind. Let us now make the change of variables $\rho' = \xi a$. Upon making this change, Eq. (3) can be rewritten in terms of two dimensionless variables u and v as

$$U(\rho,z) = -iu U_o e^{ikz} e^{iv^2/2u} \int_0^1 e^{iu\xi^2/2} J_0(v\xi)\xi d\xi, \tag{4}$$

where

$$u = 2\pi N, \quad v = 2\pi N \rho/a, \tag{5}$$

and N is the Fresnel number of the aperture at the on-axis observation point,

$$N = a^2/\lambda z. \tag{6}$$

Let us now put Eq. (4) into a form more suitable for calculations. It is shown in Sect. 14.A that in the lit region (where $\rho < a$ and hence $v < u$) the integral on the right-hand side of Eq. (4) can be expressed as

$$\int_0^1 e^{iu\xi^2/2} J_0(v\xi)\xi d\xi = \frac{i}{u}\left\{e^{-iv^2/2u} - e^{iu/2}[V_0(u,v) - iV_1(u,v)]\right\}, \tag{7}$$

where $V_0(u,v)$ and $V_1(u,v)$ are Lommel functions of two variables:

$$V_n(u,v) = \sum_{s=0}^{\infty}(-1)^s \left(\frac{v}{u}\right)^{2s+n} J_{2s+n}(v). \tag{8}$$

Upon substituting the right-hand side of Eq. (7) into Eq. (4), the field in the lit region attains the form

$$U(\rho,z) = U_o e^{ikz} M(\rho,z), \tag{9}$$

where

$$M(\rho,z) = 1 - e^{iu/2} e^{iv^2/2u}[V_0(u,v) - iV_1(u,v)]. \tag{10}$$

Equation (9) shows that the diffracted complex amplitude is the product of the incident field amplitude $U_o e^{ikz}$ (i.e., the total field if no aperture were present), and the function $M(\rho,z)$. We shall therefore refer to $M(\rho,z)$ as the *modifier* function, since it describes how the presence of the aperture modifies the field.

The intensity, $I(\rho,z)$, of the field in the lit region is given by

$$I(\rho,z) = U(\rho,z)^* U(\rho,z) = I_o |M(\rho,z)|^2, \tag{11}$$

where * denotes the complex conjugate and $I_o = |U_o|^2$ is the intensity of the incident field. It follows from Eq. (9) that the phase $\phi(\rho,z)$ of the field is given by

$$\phi(\rho,z) = kz + \psi(\rho,z), \tag{12}$$

where

$$\psi(\rho,z) = \arg M(\rho,z), \tag{13}$$

and arg denotes the argument of the complex-valued function $M(\rho,z)$. We shall refer to $\psi(\rho,z)$ as the reduced phase.

14.2.1.2 On-axis intensity and phase

Let us first examine the intensity and phase at on-axis observation points. At such points, $\rho = 0$ and hence $v = 0$. It follows directly from Eq. (8) that $V_0(u,0) = 1$ and $V_1(u,0) = 0$. We then find from Eq. (10) that the on-axis modifier function is

$$M(0,z) = 1 - e^{iu/2} = 1 - e^{iN\pi}, \tag{14}$$

where the z-dependence enters through the Fresnel number N. It then follows from Eq. (11) that the on-axis intensity is given by

$$I(0,z) = I_o \left|1 - e^{iN\pi}\right|^2 = 4I_o \sin^2(N\pi/2). \tag{15}$$

This function is plotted in Fig. 2 over the interval $1 \leq N \leq 6$. When the Fresnel number is odd, the intensity is maximum with a value of $I(0,z) = 4I_o$. We will refer to the corresponding observation points as *focal points*. When the Fresnel number is even we have $I(0,z) = 0$, and we will refer to the corresponding observation points as *singular points* because the modulus of the complex amplitude $U(0,z)$ is zero at such points, and hence its phase is undefined there [10,11].

The expression for the reduced phase can be obtained from Eqs. (13) and (14), and we find that

$$\psi(0,z) = \arg(1 - e^{iN\pi}). \tag{16}$$

This function is plotted in Fig. 3 over the interval $1 \leq N \leq 6$. Note that the phase jumps by π as we pass through the singular points $N = 2$, 4 and 6.

14.2.1.3 General case

In this section, the intensity and reduced phase in observation planes at a variety of distances from the aperture will be investigated. For the sake of comparison, let us first recall the paraxial form for a diverging spherical wave. A spherical wave emanating from the origin and arriving at the position P in Fig. 1 is described by the wave function $\exp(ikr)/r$, where $r = (\rho^2 + z^2)^{1/2}$. The paraxial approximation to this function is $\exp(ikr)/r \approx \exp[ik(z + \rho^2/2z)]/z$. Upon comparing this equation to Eq. (9), we see that the paraxial approximation to the reduced phase of this

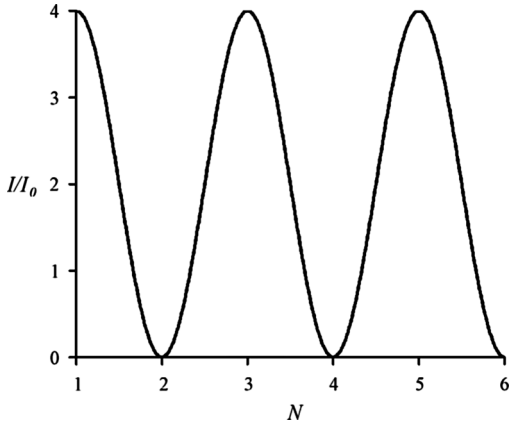

Figure 2 The on-axis intensity I, in units of I_o, as a function of the Fresnel number N.

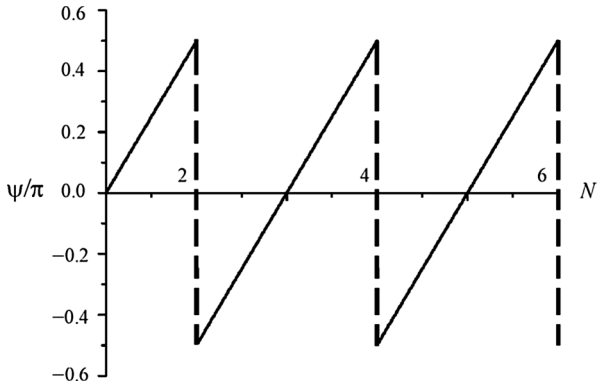

Figure 3 The on-axis reduced phase ψ, in units of π, as a function of the Fresnel number N.

wave is

$$\psi(\rho, z) \approx k\rho^2/2z. \tag{17}$$

The intensity and reduced phase of the diffracted field along the x-axis in several observation planes at different distances from the aperture plane are plotted in Figs. 4 and 5. The behavior of the field as we travel outward from the aperture plane and pass through a focal point is depicted in Figs. 4(a) through 4(c). In Fig. 4(a) the Fresnel number is 3.5, and in this plane we see that the reduced phase near the axis has a curvature with the opposite sign of that of the phase in Eq. (17). Hence the wave in this plane corresponds to a converging wave. The on-axis intensity value is approximately 2.0. In Fig. 4(b) the Fresnel number is 3. This is a focal plane, and we see that the reduced phase is constant near the axis, i.e., the wave is behaving like a plane wave in this region. The on-axis intensity value in this case is 4.0. In Fig. 4(c) the Fresnel number is 2.5, and we see that in this plane the reduced phase near the axis has a curvature with the same sign as the phase in Eq. (17). Hence the wave corresponds to a diverging wave. The on-axis intensity value is approximately 2.0.

As we move further away from the aperture plane, the wave near the axis diverges more strongly, until we reach the on-axis point where the Fresnel number is 2.0. At this point the intensity of the field is zero, and its phase is undefined. Such a point is referred to as a singular point of the field. Figure 4(d) shows the intensity and phase of the wave in the plane where the Fresnel number is 2.01, i.e., just before we reach the singular point. The phase near the axis has a steep upward curvature, corresponding to a strongly diverging wave. The value of the phase on-axis is approximately $-\pi/2$. Figure 5(a) shows the intensity and phase of the wave in the plane where the Fresnel number is 1.99, i.e., just after we have passed through the singular point. The phase near the axis has a steep downward

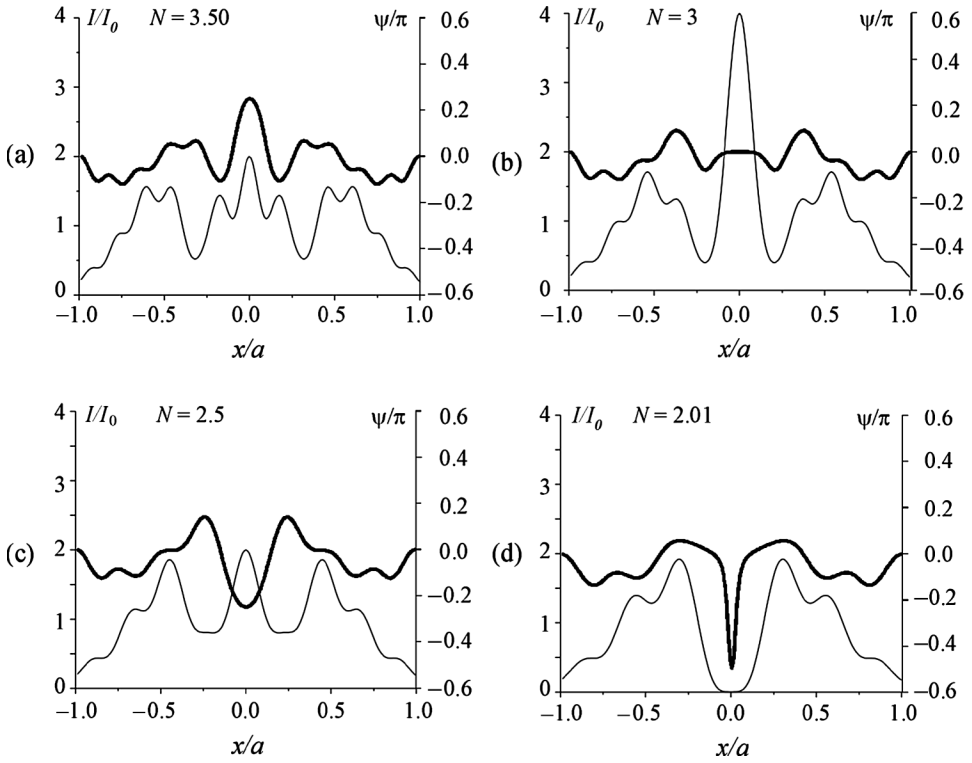

Figure 4 Plots of I/I_o (thin line) and ψ/π (thick line) as functions of position along the x-axis for observation planes with Fresnel numbers: (a) $N = 3.5$, (b) $N = 3$, (c) $N = 2.5$, and (d) $N = 2.01$.

curvature, corresponding to a strongly converging wave. The on-axis value of the phase here is approximately $\pi/2$, so as we pass through the singular point, the phase jumps by π. Figure 5(b) shows that as we continue to move further away from the aperture plane, the field near the axis starts to converge less strongly. Finally, at the next focal point, the plane where $N = 1.0$, we see that the phase near the axis is again constant; and hence the wave is again behaving like a plane wave. This is shown in Fig. 5(c). In addition, by comparing Fig. 5(c) to Fig. 4(b), we see that for focal points further from the aperture plane, the wavefront is planar over a larger area in the observation plane.

Figure 6 shows the lines of constant phase, ϕ, in the xz-plane near the $N = 2$ singular point, for the case $a/\lambda = 50$. It is evident from the figure that as the wave approaches the singular point, it is a diverging wave whose radius of curvature becomes smaller and smaller. It also follows from the figure that after the wave has passed through the singular point, it is now a *converging* wave whose radius of curvature is increasing.

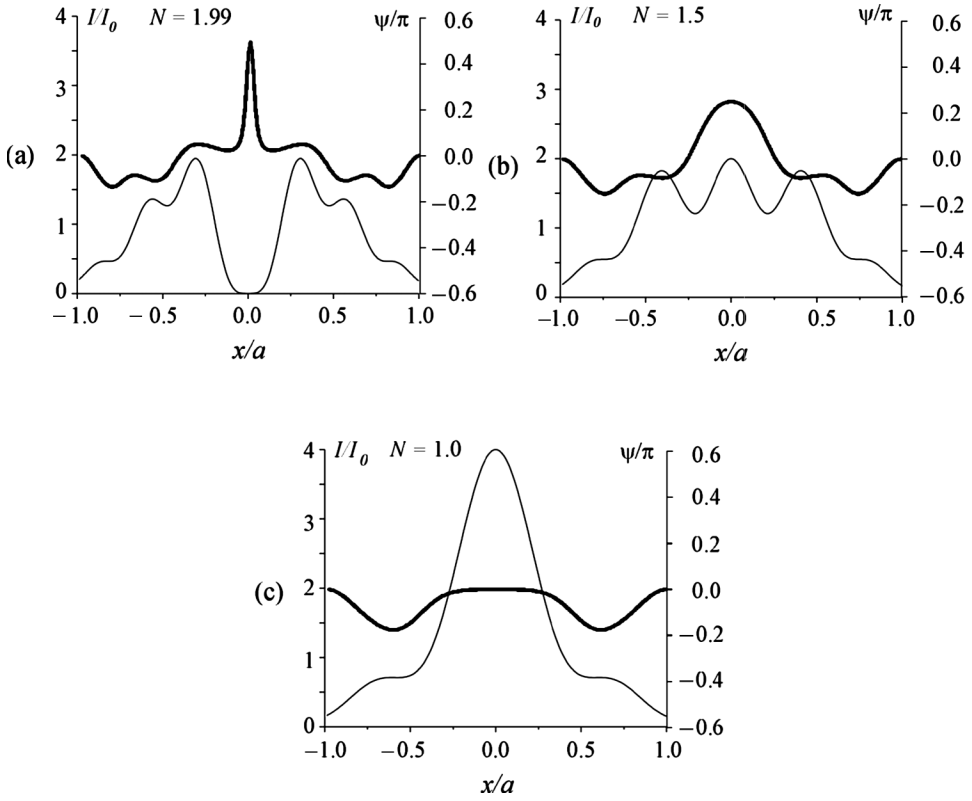

Figure 5 Plots of I/I_o (thin line) and ψ/π (thick line) as functions of position along the x-axis for observation planes with Fresnel numbers: (a) $N = 1.99$, (b) $N = 1.5$, and (c) $N = 1.0$.

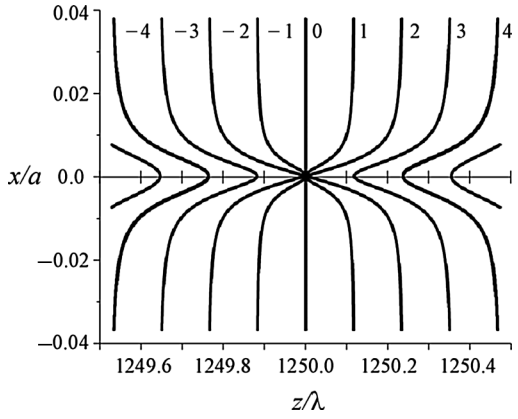

Figure 6 Lines of constant phase, ϕ, in the xz-plane near the $N = 2$ singular point when $a/\lambda = 50$. The transverse coordinate x is in units of a, and the z-coordinate is in units of the wavelength λ. The value of the phase for each line is labeled in units of $\pi/4$.

14.2.2 Incident Gaussian beam

14.2.2.1 Basic equations

Let the incident field be a Gaussian beam whose waist occurs at the aperture plane $z = 0$. The complex amplitude of the incident field is

$$U^{(i)}(\rho, \theta, z) = U_o \frac{w_o}{w} e^{i(kz-\chi)} e^{ik\rho^2/2R} e^{-\rho^2/w^2}, \tag{18}$$

where U_o is a positive constant and w_o is the spot size of the beam waist. Here, w is the spot size in the plane $z =$ constant,

$$w = w_o \sqrt{1 + (z/z_R)^2}, \tag{19}$$

R is the radius of curvature in that plane,

$$R = z + \frac{z_R^2}{z}, \tag{20}$$

χ is the Gouy phase

$$\tan\chi = \frac{z}{z_R}, \tag{21}$$

and $z_R = \pi w_o^2/\lambda$ is the Rayleigh length of the beam. It follows from Eqs. (18)–(21) that the complex amplitude in the plane $z = 0$ is

$$U^{(i)}(\rho', \theta', 0) = U_o e^{-\rho'^2/w_o^2}. \tag{22}$$

In order to find the field at the observation point $P = (\rho, \theta, z)$, we substitute the incident field into Eq. (2). After performing the angular integration, we find that the complex amplitude of the field is independent of θ and is given by the expression

$$U(\rho, z) = \frac{k}{iz} U_o e^{ikz} e^{ik\rho^2/2z} \int_0^a e^{-\rho'^2/w_o^2} e^{ik\rho'^2/2z} J_0(k\rho\rho'/z)\rho' d\rho'. \tag{23}$$

Let us now make the change of variables $\rho' = \xi a$. Upon making this change, Eq. (23) can be rewritten in terms of two dimensionless variables u and v as

$$U(\rho, z) = -iU_o 2\pi N e^{ikz} e^{iN\pi(\rho/a)^2} \int_0^1 e^{iu\xi^2/2} J_0(v\xi)\xi, d\xi, \tag{24}$$

where

$$u = 2\pi N + 2i\beta^2, \quad v = 2\pi N(\rho/a). \tag{25}$$

Here, N is the Fresnel number of the aperture at an on-axis observation point, given by Eq. (6), and

$$\beta = a/w_o. \tag{26}$$

We will refer to β as the aperture-spot ratio since its numerical value specifies how many beam spots would fit across the aperture.

If we now substitute the right-hand side of Eq. (7) into Eq. (24), we find that the complex amplitude is

$$U(\rho,z) = U_o e^{ikz} G(\rho,z), \tag{27}$$

where

$$G(\rho,z) = \frac{2\pi N}{u} e^{iN\pi(\rho/a)^2} e^{-iv^2/2u} M(\rho,z), \tag{28}$$

and $M(\rho,z)$ is given by Eq. (10). Note, however, that in the present case the variable u on the right-hand side of Eq. (10) is a complex value [see Eq. (25)]. The intensity of the field in the lit region is given by

$$I(\rho,z) = |U(\rho,z)|^2 = I_o |G(\rho,z)|^2, \tag{29}$$

where $I_o = |U_o|^2$ is the on-axis incident intensity in the plane $z = 0$. It follows from Eq. (28) that the phase of the field is

$$\phi(\rho,z) = kz + \psi(\rho,z), \tag{30}$$

where

$$\psi(\rho,z) = \arg G(\rho,z). \tag{31}$$

As before, we shall refer to $\psi(\rho,z)$ as the reduced phase.

Equation (27) is a useful way of writing the complex amplitude of the diffracted field, especially for calculations, but there is an alternative representation that is interesting. It is shown in Sect. 14.B that

$$\frac{2\pi N}{u} = \frac{w_o}{w} e^{-i\chi}, \tag{32}$$

and that

$$e^{iN\pi(\rho/a)^2}e^{-iv^2/2u} = e^{ik\rho^2/2R}e^{-\rho^2/w^2}. \tag{33}$$

After substituting the right-hand side of this equation into Eq. (28), and then substituting that result into Eq. (27) we obtain

$$U(\rho,z) = U_o\frac{w_o}{w}e^{i(kz-\chi)}e^{ik\rho^2/2R}e^{-\rho^2/w^2}M(\rho,z), \tag{34}$$

which is

$$U(\rho,z) = U^{(i)}(\rho,\theta,z)M(\rho,z), \tag{35}$$

with $U^{(i)}(\rho,\theta,z)$ given by Eq. (18). Equation (35) shows that the diffracted complex amplitude is the product of the incident field complex amplitude and the function $M(\rho,z)$. Hence, as in the previous section, we shall refer to $M(\rho,z)$ as the modifier function, since it describes how the presence of the aperture modifies the field.

14.2.2.2 On-axis intensity and phase

Let us now examine the intensity and phase at on-axis observation points. At such points, $\rho = 0, v = 0$, and the corresponding modifier function is given by

$$M(0,z) = 1 - e^{iu/2} = 1 - e^{iN\pi}e^{-\beta^2}. \tag{36}$$

It then follows from Eqs. (29) and (28) that

$$I(0,z) = I_o|G(0,z)|^2 = I_o\frac{4\pi^2N^2}{|u|^2}|M(0,z)|^2 = I_o\frac{4\pi^2N^2}{|u|^2}\left|1 - e^{iN\pi}e^{-\beta^2}\right|^2, \tag{37}$$

where u is given by Eq. (25).

Figure 7 depicts the on-axis intensity as a function of the Fresnel number for four different values of the aperture-spot ratio. In all four cases the intensity

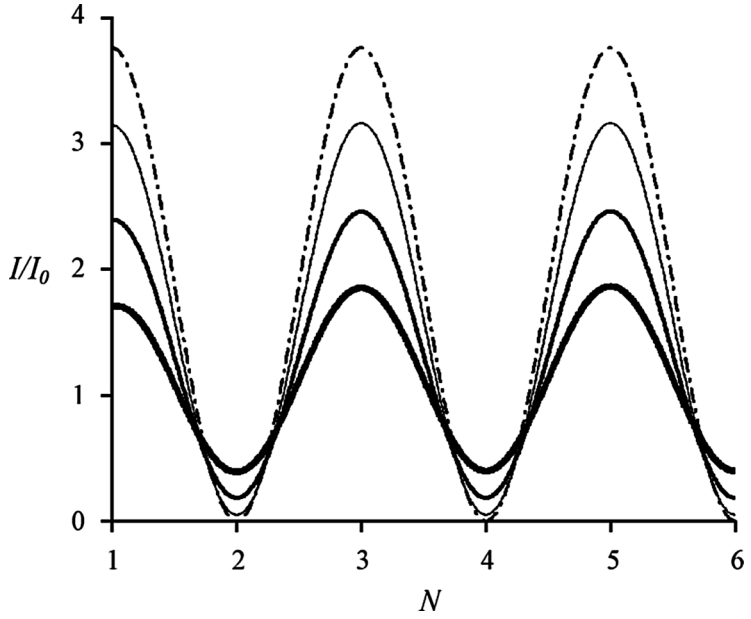

Figure 7 The on-axis intensity I, in units of I_o, for $\beta = 0.25$ (dashed line), $\beta = 0.50$ (thin solid line), $\beta = 0.75$ (medium solid line), and $\beta = 1.0$ (thick solid line).

is maximum (minimum) when the Fresnel number is approximately odd (even). These plots show that as the aperture-spot ratio increases, the focusing effect becomes weaker: the values of the maximum intensity decrease (as compared to the value of 4 for the case of an incident plane wave) and the values of the minimum intensity increase (with respect to the value of zero for the incident plane wave).

It follows from Eqs. (35) and (36) that the on-axis field is

$$U(0,z) = U_o \frac{w_o}{w} e^{i(kz-\chi)} \left(1 - e^{iN\pi} e^{-\beta^2}\right). \tag{38}$$

The on-axis reduced phase is therefore

$$\psi(0,z) = \arg\left[e^{-i\chi}\left(1 - e^{iN\pi} e^{-\beta^2}\right)\right]. \tag{39}$$

It is interesting to notice that when the Fresnel number is an integer, we have $\psi(0,z) = -\chi$. Figure 8 shows the on-axis reduced phase as a function of the Fresnel number for the same four values of the aperture-spot ratio as in Fig. 7. As the aperture-spot ratio is increased, the size of the phase change decreases.

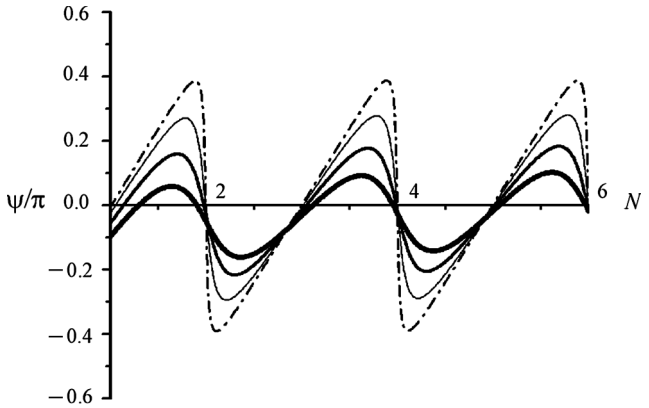

Figure 8 The on-axis reduced phase ψ, in units of π, for $\beta = 0.25$ (dashed line), $\beta = 0.50$ (thin solid line), $\beta = 0.75$ (medium solid line), and $\beta = 1.0$ (thick solid line).

14.2.2.3 General case

The intensity and reduced phase of the diffracted field along the x-axis in several observation planes are plotted in Fig. 9, for the case $\beta = 0.57$, i.e., $a = 0.57w_o$. The behavior of the field as we travel outward from the aperture plane and pass through a focal plane is depicted in Figs. 9(a) through 9(c). In Fig. 9(a) the Fresnel number is 3.5. The downward curvature of the phase near the axis shows that the wave is converging in that region. In Fig. 9(b) the Fresnel number is 3. The phase is constant near the axis, and hence the wavefront is planar in this region. In Fig. 9(c) the Fresnel number is 2.5. The upward curvature of the phase shows that the wave is diverging in this region. The qualitative behavior of the intensity and phase pictured in Figs. 9(a)–(c) is very similar to the behavior of the intensity and phase in the plane wave case [see Figs. 4(a)–(c)]. The main difference is that the peak intensity in the $N = 3$ focal plane is 2.96 in the present case, and was 4 in the plane wave case.

As we move further away from the aperture plane, the field continues to diverge, until we approach the on-axis position where $N = 2$ [Fig. 9(d)]. The intensity then goes through a minimum, and the character of the wave changes from diverging to converging as we pass through this point. The behavior is similar to that seen at the position where $N = 2$ in the plane wave case. The present behavior is different in that the phase varies continuously as we pass through this point (see Fig. 8), instead of discontinuously, as it did in the plane wave case (see Fig. 3).

As we get further away from the aperture plane the wave becomes converging again. This is illustrated by the plot of the phase in Fig. 9(e), where $N = 1.5$. The downward curvature of the phase near the axis means that the wave is converging in this region. As we approach the point where $N = 1$, the wavefront flattens out.

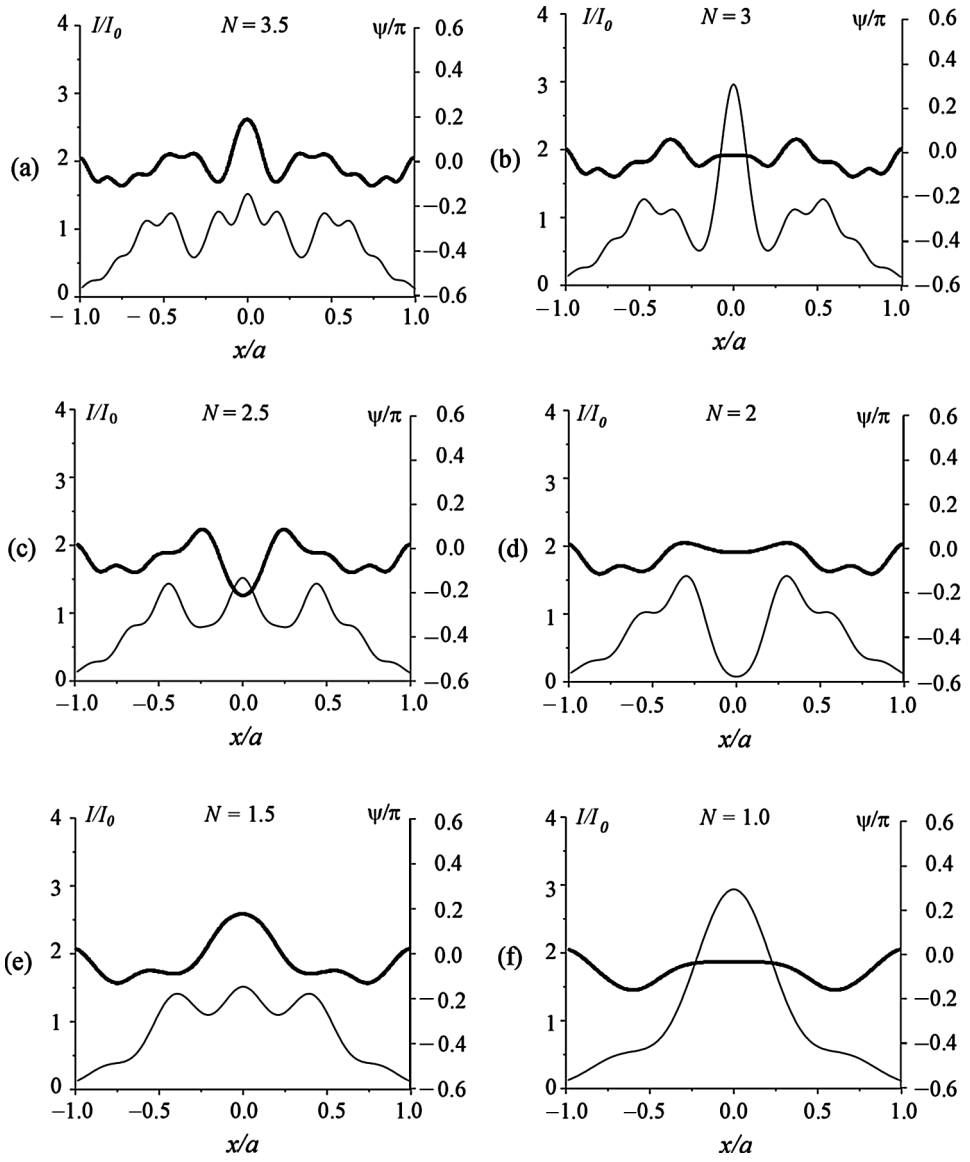

Figure 9 Plots of I/I_o (thin line) and ψ/π (thick line) as functions of position along the x axis for observation planes with Fresnel numbers: (a) $N = 3.5$, (b) $N = 3$, (c) $N = 2.5$, (d) $N = 2$, (e) $N = 1.5$, and (f) $N = 1$. The parameter β is 0.57.

Figure 9(f) shows that the phase is constant near the axis when $N = 1$; therefore the wavefront is planar in this region. The character of the wave as we move from the plane $N = 1.5$ to the plane $N = 1$ is similar to that in the plane wave case. The major difference is that the peak intensity at the $N = 1$ plane here is 2.94, whereas for the case of a plane wave it was 4.

14.3 Fresnel Diffraction by a Bicomponent System of Apertures

14.3.1 Incident plane wave

14.3.1.1 Basic equations

Let us now consider the two-aperture system depicted in Fig. 10. The radius of the first aperture is a_1, the radius of the second aperture is a_2, and the distance between the planes containing the apertures is L. Let $P'' = (x'', y'', L)$ be a point inside the second aperture, and $P = (x, y, z)$ be an observation point in the plane $z =$ constant $> L$. In cylindrical polar coordinates we then write $P'' = (\rho'', \theta'', L)$ and $P = (\rho, \theta, z)$. It follows from Eqs. (9) and (10) that the complex amplitude of the field incident upon the second aperture is given by

$$U(\rho'', \theta'', L) = U_o e^{ikL} \left\{ 1 - e^{iu_1/2} e^{iv_1^2/2u_1} \left[V_0(u_1, v_1) - iV_1(u_1, v_1) \right] \right\}, \qquad (40)$$

where $u_1 = 2\pi N_1, v_1 = 2\pi N_1 \rho''/a_1$ and $N_1 = a_1^2/\lambda L$.

In order to compare our results for the intensity to those of Ref. [4], we now assume that the distance L is such that N_1, the Fresnel number of the first aperture at the center of the second aperture, is equal to unity. In this case, $u_1 = 2\pi$,

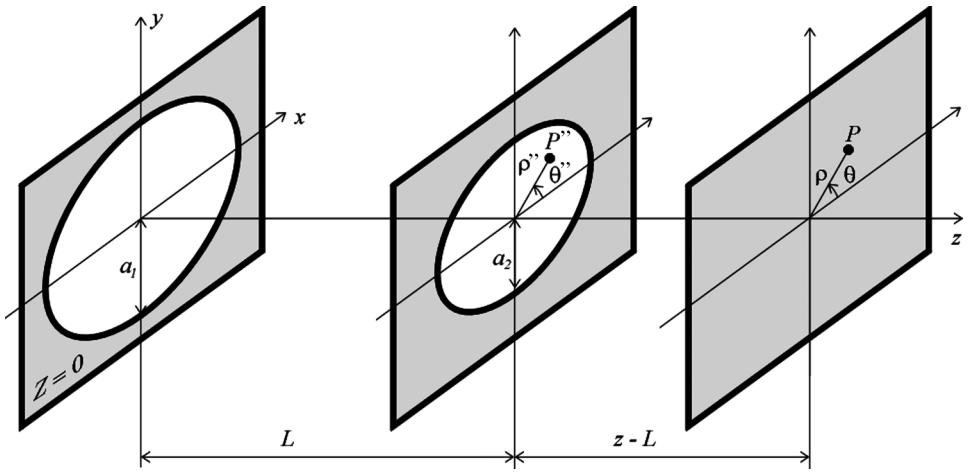

Figure 10 Geometry for the diffraction of a plane wave by a system of two circular apertures with radii a_1 and a_2, respectively. The distance between the two aperture planes is L. Point $P'' = (\rho'', \theta'', L)$ is a point inside the second aperture and $P = (\rho, \theta, z)$ is a point in the observation plane $z =$ constant.

$v_1 = 2\pi\rho''/a_1$ and Eq. (40) can be written as

$$U(\rho'', \theta'', L) = U_o e^{ikL}\left[1 + D(\rho''/a_1)\right], \tag{41}$$

where

$$D(w) = e^{i\pi w^2}\left[V_0(2\pi, 2\pi w) - iV_1(2\pi, 2\pi w)\right]. \tag{42}$$

Let us now investigate the complex amplitude, $U(\rho, \theta, z)$, of the diffracted field in the region $z > L$. The paraxial form of the Fresnel approximation to the Rayleigh-Sommerfeld diffraction formula tells us that this field is given by the expression

$$U(\rho, \theta, z) = \frac{k}{2\pi i(z-L)} e^{ik(z-L)} e^{ik\rho^2/2(z-L)} \times \int_0^{a_2}\int_0^{2\pi} U(\rho'', \theta'', L) e^{ik\rho''^2/2(z-L)} e^{-ik\rho\rho''\cos(\theta-\theta'')/(z-L)} \rho'' d\rho'' d\theta''. \tag{43}$$

Upon substituting the right-hand side of Eq. (41) into Eq. (43) and performing the angular integration, we find that the field is independent of the angle θ and given by

$$U(\rho, z) = \frac{k}{i(z-L)} U_o e^{ikz} e^{ik\rho^2/2(z-L)} \times \int_0^{a_2} \left[1 + D(\rho''/a_1)\right] e^{ik\rho''^2/2(z-L)} J_0\left[k\rho\rho''/(z-L)\right] \rho'' d\rho''. \tag{44}$$

Let us now make the change of variable $\rho'' = \xi a_2$. After using this relation in the right-hand side of Eq. (44), we find that the field can be described in terms of the dimensionless variables u_2 and v_2 as

$$U(\rho, z) = -iu_2 U_o e^{ikz} e^{iv_2^2/2u_2} \int_0^1 [1 + D(\alpha\xi)] e^{iu_2\xi^2/2} J_0(v_2\xi)\xi d\xi, \tag{45}$$

where

$$u_2 = 2\pi N_2, \quad v_2 = 2\pi N_2 \rho''/a_2, \tag{46}$$

with N_2 the Fresnel number of the second aperture at the on-axis point in the observation plane,

$$N_2 = a_2^2/\lambda(z-L), \tag{47}$$

and α the ratio of the radii of the two apertures,

$$\alpha = a_2/a_1. \tag{48}$$

By analogy with the results of Sect. 14.2, let us write Eq. (45) as

$$U(\rho,z) = U_o e^{ikz} M(\rho,z), \tag{49}$$

where

$$M(\rho,z) = -iu_2 e^{iv_2^2/2u_2} \int_0^1 [1 + D(\alpha\xi)] e^{iu_2\xi^2/2} J_0(v_2\xi)\xi d\xi. \tag{50}$$

It follows from Eq. (49) that the intensity and phase of the field in the lit region are given, respectively, by Eqs. (11) and (12), with $M(\rho,z)$ given by Eq. (50) and the reduced phase defined as in Eq. (13). The function $M(\rho,z)$ can be evaluated by numerical integration.

14.3.1.2 On-axis intensity and phase

The on-axis intensity and reduced phase of the field after the second aperture were calculated by the method described above, and are plotted as a function of the Fresnel number N_2 for $\alpha = 0.1$ in Fig. 11, and for $\alpha = 0.5$ in Fig. 12. One general comment is in order before discussing the results. There are no true singular points behind the second aperture, because even at points where the intensity is minimum, its value is not exactly zero.

Figures 11 and 12 show the results for $\alpha = 0.1$ and 0.5, respectively. In both cases the values of the intensity and the reduced phase oscillate as functions of N_2. Upon comparing the two sets of curves, we see that three changes occur when α is increased from 0.1 to 0.5. First, the maximum value of the on-axis intensity decreases (from approximately $15I_o$ to $8I_o$), and the minimum value increases (from approximately zero to I_o). Second, the amplitude of the oscillation of the reduced phase decreases and does not occur so suddenly. Finally, at the smaller value of α the maxima (minima) of the intensity occur when the Fresnel number is odd (even), but at the larger value they are shifted to slightly higher values of N_2; likewise the reduced phase curve is also shifted toward higher values of N_2.

The explanation for this behavior is as follows. When $\alpha = 0.1$, the radius of the second aperture is 10 times smaller than that of the first. In this case the results of Sect. 14.2 show that the phase of the field incident upon the second aperture is constant across it [see Fig. 5(c)], and that the value of the intensity incident upon it varies by only 10% across it. Therefore the field incident upon the second aperture is very similar to the field incident upon the first aperture (a constant

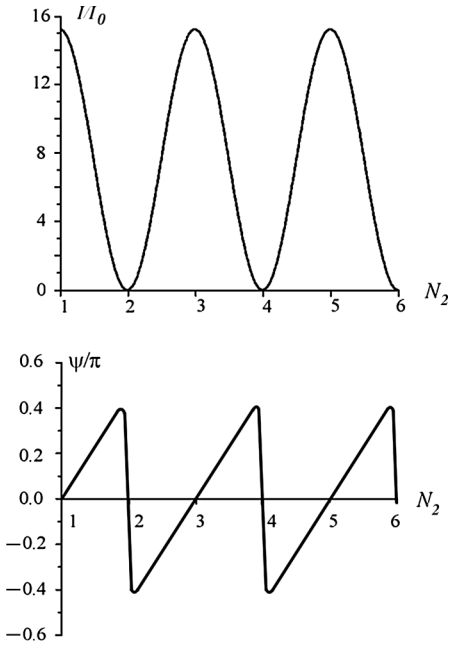

Figure 11 Plots of I/I_o and ψ/π for on-axis observation points as functions of the Fresnel number N_2 for $\alpha = 0.1$.

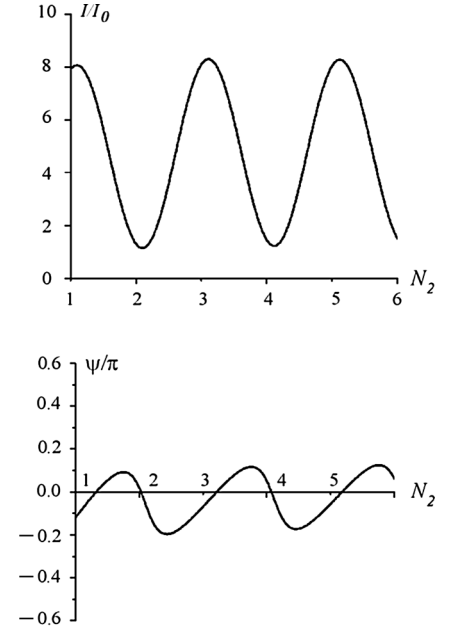

Figure 12 Plots of I/I_o and ψ/π for on-axis observation points as functions of the Fresnel number N_2 for $\alpha = 0.5$.

amplitude, normally incident plane wave), and this explains why the second aperture increases the on-axis intensity at the focal points by a factor of close to four, why the intensities at the minima are approximately zero, and why the phase jumps are approximately equal to π. As α increases from the value 0.1, the phase of the field incident upon the second aperture remains approximately constant across it, but the intensity begins to vary considerably. As a result, the effect of the second aperture becomes less ideal. When $\alpha = 0.5$, as in Fig. 12, both the phase and the intensity of the field incident upon the second aperture vary significantly across it [see Fig. 5(c)], and the effect of the second aperture is correspondingly less ideal.

14.3.1.3 General case

The intensity and reduced phase of the diffracted field as a function of the scaled transverse coordinate x/a_2 in six different planes behind the second aperture are shown in Fig. 13 for the case $\alpha = 0.4$. In Fig. 13(a) the value of the Fresnel number, $N_2 = 3.06$, was chosen such that the on-axis intensity was maximum, i.e., so that the plane is a focal plane. We see from the figure that the phase near the axis is approximately constant, so that the wave in that region is behaving like a plane wave. In Figs. 13(b) and 13(c) the Fresnel numbers are 2.5 and 2.37, respectively, and the wave is diverging in each case. In Fig. 13(d) the Fresnel number is 1.74, and the wave has changed from a diverging wave to a converging wave, i.e., it has refocused. In Fig. 13(e) the Fresnel number is 1.5, and the wave continues to converge. In Fig. 13(f) the Fresnel number is 1.05, and the plane is a focal plane. The on-axis intensity is maximum, and the phase near the axis is approximately constant. In Ref. [4] the value of α was 0.4, as it is in Fig. 13. Our results for the intensities agree well with those of Ref. [4].

14.3.2 Incident Gaussian beam

14.3.2.1 Basic equations

It follows from Eqs. (27), (28), and (10) that the complex amplitude of the field incident upon the second aperture is

$$U(\rho'', L) = U_o e^{ikL} H(\rho''/a_1), \tag{51}$$

where

$$H(w) = \frac{2\pi N_1}{u_1} e^{iN_1 \pi w^2} \left\{ e^{-iv_1^2/2u_1} - e^{iu_1/2} \left[V_0(u_1, v_1) - iV_1(u_1, v_1) \right] \right\}. \tag{52}$$

Here,

$$u_1 = 2\pi N_1 + 2i\beta^2, \quad v_1 = 2\pi N_1 w, \tag{53}$$

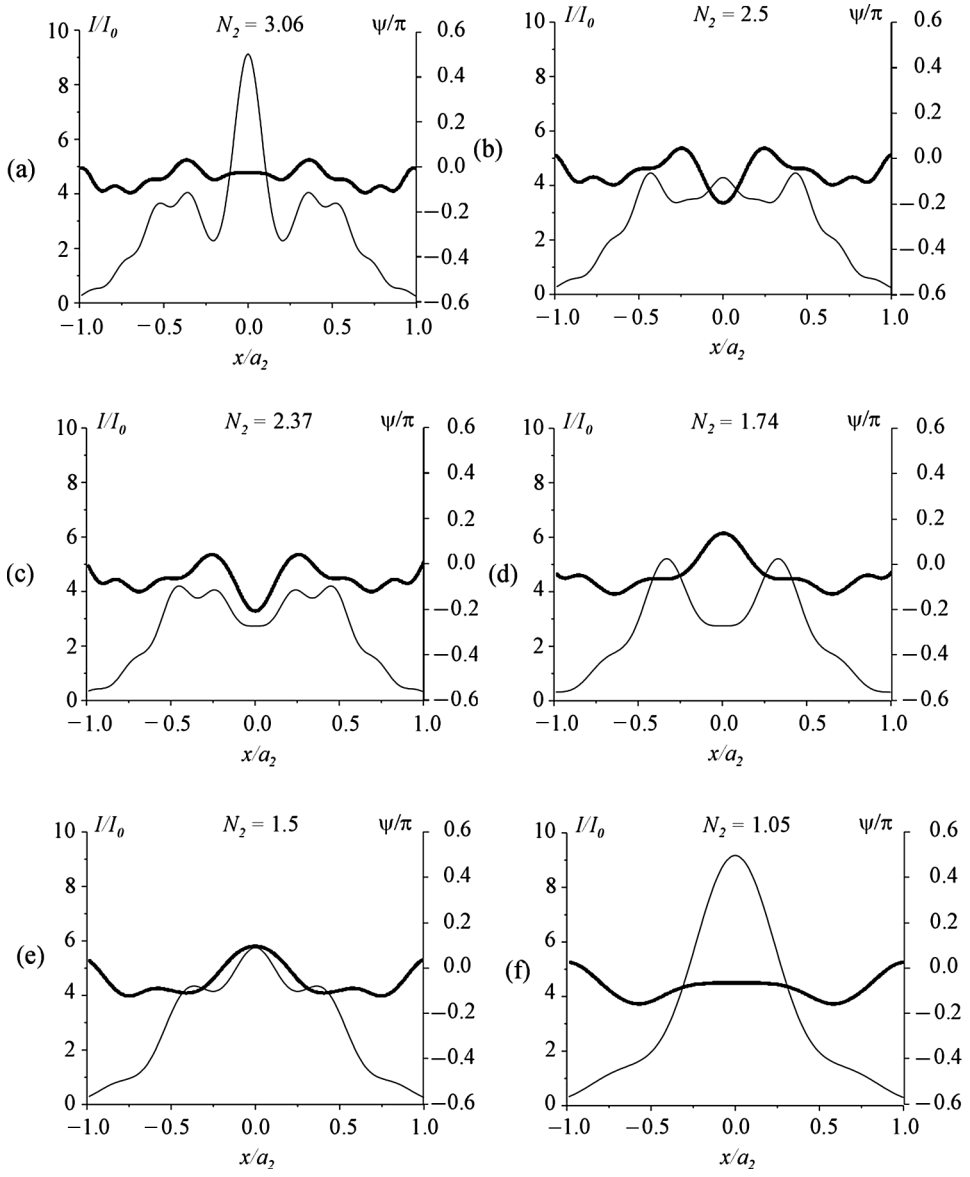

Figure 13 Plots of I/I_o (thin line) and ψ/π (thick line) as functions of position along the x-axis for observation planes behind the second aperture with Fresnel numbers: (a) $N_2 = 3.06$, (b) $N_2 = 2.5$, (c) $N_2 = 2.37$, (d) $N_2 = 1.74$, (e) $N_2 = 1.5$, and (f) $N_2 = 1.05$.

and N_1 is the Fresnel number of the first aperture at the observation point at the center of the second aperture,

$$N_1 = a_1^2/\lambda L. \tag{54}$$

As in the previous section, let $N_1 = 1$. Equation (52) then simplifies to

$$H(w) = \frac{2\pi}{u_1} e^{i\pi w^2} \left\{ e^{-iv_1^2/2u_1} - e^{iu_1/2} [V_0(u_1, v_1) - iV_1(u_1, v_1)] \right\}, \tag{55}$$

where $u_1 = 2\pi + 2i\beta^2$, and $v_1 = 2\pi w$. In order to find the field at the observation point $P = (\rho, \theta, z)$ we substitute this incident field into Eq. (43). Upon performing the angular integration, we find that the field is independent of the angle θ and that

$$U(\rho, z) = \frac{k}{i(z-L)} U_o e^{ikz} e^{ik\rho^2/2(z-L)} \times \int_0^{a_2} H(\rho''/a_1) e^{ik\rho''^2/2(z-L)} J_0 [k\rho\rho''/(z-L)] \rho'' d\rho''. \tag{56}$$

Let us now make the change of variable $\rho'' = \xi a_2$. After substituting this relation into the right-hand side of Eq. (56), we find that the field can be described in terms of the dimensionless variables u_2 and v_2 as

$$U(\rho, z) = -iu_2 U_o e^{ikz} e^{iv_2^2/2u_2} \int_0^1 H(\alpha\xi) e^{iu_2\xi^2/2} J_0(v_2\xi) \xi d\xi, \tag{57}$$

where

$$u_2 = 2\pi N_2, \quad v_2 = 2\pi N_2 \rho / a_2. \tag{58}$$

Here, N_2 is the Fresnel number of the second aperture at the observation point (ρ, θ, z),

$$N_2 = a_2^2/\lambda(z-L), \tag{59}$$

and α is the ratio of the radii of the two apertures [see Eq. (48)]. By analogy with the results of the previous subsection, let us write Eq. (57) as

$$U(\rho, z) = U_o e^{ikz} G(\rho, z), \tag{60}$$

where

$$G(\rho, z) = -iu_2 e^{iv_2^2/2u_2} \int_0^1 H(\alpha\xi) e^{iu_2\xi^2/2} J_0(v_2\xi) \xi d\xi. \tag{61}$$

It follows from Eq. (60) that the intensity and phase of the field in the lit region are given by Eqs. (29) and (30), respectively, with $G(\rho, z)$ given by Eq. (61) and

the reduced phase defined as in Eq. (31). The function $G(\rho,z)$ can be evaluated by numerical integration.

14.3.2.2 On-axis intensity and phase

The on-axis intensity and phase behind the second aperture were calculated using the methods described above. Figure 14 shows plots of the on-axis intensity as a function of N_2 for: (a) an incident plane wave (which corresponds to $\beta = 0$), (b) an incident Gaussian beam with aperture-spot ratio of $\beta = 0.57$, and (c) an incident Gaussian beam with an aperture-spot ratio of $\beta = 1$. In all three cases the value of the ratio of the two aperture radii is $\alpha = 0.4$. The qualitative behavior of the three curves is very similar, but there are some differences. The peak intensity decreases as β is increased. This is to be expected, since a larger β corresponds to an amplitude distribution in the first aperture that is further from a uniform amplitude situation. Secondly, as β is increased, the curves shift toward a lower Fresnel number, i.e., toward the aperture. Finally, the minima are lower for the larger β cases.

Figure 15 shows plots of the on-axis reduced phase as a function of N_2 for $\beta = 0, 0.57$, and 1. The qualitative behavior of the three curves is very similar. However, as β increases, the curves shift toward lower values of the Fresnel number, and are shifted downward in numerical value.

14.3.2.3 General case

The intensity and reduced phase of the diffracted field as a function of the scaled transverse coordinate x/a_2 in four different planes behind the second aperture are

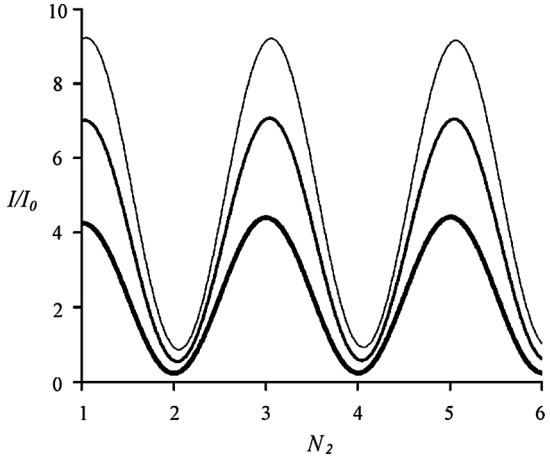

Figure 14 The on-axis intensity $I(0,z)$, in units of I_o, as a function of the Fresnel number of the second aperture, N_2, for $\beta = 0$ (thin line), $\beta = 0.57$ (medium thick line), and $\beta = 1$ (thick line), all for $\alpha = 0.4$.

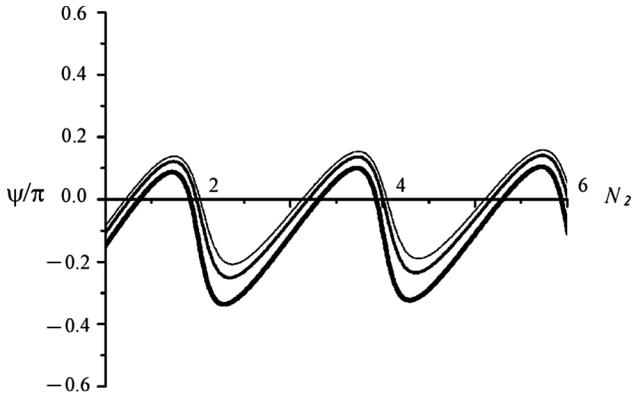

Figure 15 The on-axis reduced phase $\psi(0,z)$, in units of π, as a function of the Fresnel number of the second aperture, N_2, for $\beta = 0$ (thin line), $\beta = 0.57$ (medium thick line), and $\beta = 1$ (thick line), all for $\alpha = 0.4$.

shown in Fig. 16 for the case $\alpha = 0.4$. In Fig. 16(a) the Fresnel number is 3.04, and the plane is a focal plane. The on-axis intensity is maximum, and the phase near the axis is approximately constant. In Fig. 16(b) the Fresnel number is 2.5, and the wave is diverging. In Fig. 16(c) the Fresnel number is 1.5, and the wave has changed from a diverging wave to a converging wave. In Fig. 16(d) the Fresnel number is 1.04, and the plane is a focal plane. The on-axis intensity is maximum, and the phase near the axis is approximately constant.

Let us now compare these results to the incident plane wave results. A comparison of Figs. 16(a) and 13(a) shows that the qualitative behavior in the two cases at the $N_2 \approx 3$ focal point is very similar. The major difference is a matter of scale: the curves have similar shapes, but the maximum intensity in the Gaussian beam case is approximately $7I_o$ instead of the $9I_o$ for the plane wave case. A comparison of Figs. 16(b) and 13(b) shows that the qualitative behavior in the two cases is very similar at the location where $N_2 = 2.5$ as well. Similar results are obtained for the location where $N_2 = 1.5$ when Figs. 16(c) and 13(e) are compared. Finally, the curves for both the intensity and phase at the $N_2 \approx 1$ focal point are very similar as well [see Figs. 16(d) and 13(f)]. As with the $N_2 \approx 3$ case, the key difference is the fact that the maximum intensity in the Gaussian beam case is approximately $7I_o$ instead of $9I_o$ for the plane wave case.

14.4 Conclusions

We have investigated the intensity and phase of the diffracted field behind a circular aperture when a monochromatic plane wave is incident upon it, and when a Gaussian beam is incident upon it. We have also investigated the intensity and

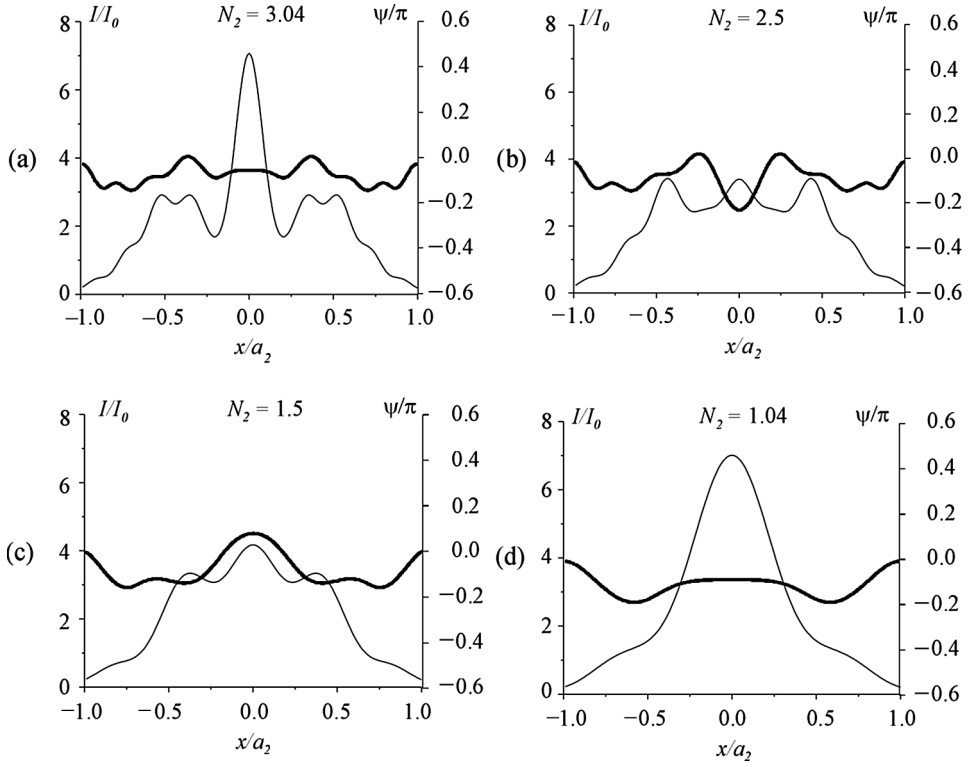

Figure 16 Plots of I/I_o (thin line) and ψ/π (thick line) as functions of position along the x-axis for observation planes after the second aperture with Fresnel numbers: (a) $N_2 = 3.04$, (b) $N_2 = 2.5$, (c) $N_2 = 1.5$, and (d) $N_2 = 1.04$.

phase of the diffracted field in a system of two circular apertures for the same incident fields.

For the single-aperture system, with a plane wave normally incident, it was shown that in the neighborhood of a focal point, the phase of the wave approaching the focal point is that of a converging wave, the phase in the focal plane is planar, and the phase of the wave exiting the focal point is that of a diverging wave. It was also shown that the wave becomes more and more divergent as the distance from the focal point is increased, until a position at which the Fresnel number becomes even is reached. At such a point the intensity of the wave is zero, and the phase of the wave is undefined, i.e., singular. It was shown that as the observation point on-axis moves away from the aperture and passes through a singular point, the nature of the wave in the neighborhood of the axis changes from that of a diverging wave to that of a converging wave, i.e., the wave refocuses.

Similar behavior was observed when a Gaussian beam was normally incident upon a circular aperture, for the case in which the waist of the Gaussian beam occurs in the plane of the aperture. It was shown that as β (the ratio of the aperture

radius to the incident beam waist) increases, the focusing effect becomes weaker, i.e., the values of the intensities at the focal points decrease. This implies that the more the incident intensity deviates from a constant value (as we had in the plane wave case), the weaker the focusing effect is.

The focusing effect was also investigated for a plane wave that was normally incident upon a two-aperture system, for the case in which the separation between the two apertures is chosen such that $N_1 = 1$. It was observed, by studying the phase, that the field focuses, defocuses, and refocuses, as in the one-aperture case. We found that the effect depended crucially on α, the ratio of the radii of the two apertures. For $\alpha = 0.1$, the focusing effect was strong, with the intensities at the focal point approximately $15I_o$. This was due to the fact that, since $N_1 = 1$, the intensity and phase of the field incident upon the second aperture were both fairly constant. As α increases and the intensity incident upon the second aperture varies across it, the focusing effect becomes weaker (the peak intensities decrease) and the positions of the focal points shift slightly. Similar behavior was also observed when a Gaussian beam was normally incident upon a two-aperture system, for the case in which the separation between the two apertures is chosen such that $N_1 = 1$. As in the single-aperture Gaussian beam case, it was found that increasing β resulted in a weaker focusing effect.

14.A Derivation of Equation (7)

It is convenient to consider the real and imaginary parts of the integral on the left-hand side of Eq. (7) separately. We set

$$\int_0^1 e^{iu\xi^2/2} J_0(v\xi)\xi\, d\xi = \tfrac{1}{2}[C(u,v) + iS(u,v)], \tag{A1}$$

where

$$C(u,v) = 2\int_0^1 \cos(u\xi^2/2) J_0(v\xi)\xi\, d\xi, \tag{A2}$$

$$S(u,v) = 2\int_0^1 \sin(u\xi^2/2) J_0(v\xi)\xi\, d\xi. \tag{A3}$$

These two integrals can be expressed in terms of the Lommel functions of two variables $V_0(u,v)$ and $V_1(u,v)$,[12]

$$C(u,v) = \frac{2}{u}\left[\sin(v^2/2u) + \sin(u/2)V_0(u,v) - \cos(u/2)V_1(u,v)\right], \tag{A4}$$

$$S(u,v) = \frac{2}{u}\left[\cos(v^2/2u) - \cos(u/2)V_0(u,v) - \sin(u/2)V_1(u,v)\right]. \tag{A5}$$

Upon substituting the right-hand sides of Eqs. (A4) and (A5) in to Eq. (A1), we find

$$\int_0^1 e^{iu\xi^2/2} J_0(v\xi)\xi\, d\xi = \frac{i}{u}\left\{e^{-iv^2/2u} - e^{iu/2}\left[V_0(u,v) - iV_1(u,v)\right]\right\}, \tag{A6}$$

which is Eq. (7).

14.B Derivation of Equations (32) and (33)

It follows from Eq. (25) that

$$\frac{u}{2\pi N} = 1 + i\frac{\beta^2}{N\pi}. \tag{B1}$$

Upon using Eqs. (6) and (26) we find that

$$\frac{u}{2\pi N} = 1 + i\frac{z}{\pi w_o^2/\lambda} = 1 + i\frac{z}{z_R} = \sqrt{1 + (z/z_R)^2}\, e^{i\chi} = \frac{w}{w_o} e^{i\chi}, \tag{B2}$$

where w and χ are given by Eqs. (19) and (21), respectively. Equation (32) is the reciprocal of Eq. (B2).

It follows from Eq. (25) that

$$\begin{aligned} i\left(\frac{N\pi\rho^2}{a^2} - \frac{v^2}{2u}\right) &= i\frac{N\pi\rho^2}{a^2}\left(1 - \frac{1}{1 + i\beta^2/N\pi}\right) = -\frac{\rho^2}{a^2}\frac{\beta^2}{1 + i\beta^2/N\pi} \\ &= -\frac{\rho^2/w_o^2}{1 + iz/z_R} = -\frac{\rho^2}{w^2} + i\frac{k\rho^2}{2R}, \end{aligned} \tag{B3}$$

where w and R are given by Eqs. (19) and (20). Equation (B3) then gives Eq. (33).

References

1. M. De, J.W.Y. Lit, and R. Tremblay, "Multi-aperture focusing technique," *Appl. Opt.* **7**, 483–488 (1968).
2. J.W.Y. Lit and R. Tremblay, "Boundary-diffraction-wave theory of cascaded-apertures diffraction," *J. Opt. Soc. Am.* **59**, 559–567 (1969).
3. J.W.Y. Lit, R. Boulay, and R. Tremblay, "Diffraction fields of a sequence of equal radii circular apertures," *Opt. Comm.* **1**, 280–282 (1970).
4. R.R. Letfullin and T.F. George, "Optical effect of diffractive multifocal focusing of radiation on a bi-component diffraction system," *Appl. Opt.* **39**, 2545–2550 (2000).

5. R.R. Letfullin and O.A. Zayakin, "Observation of the effect of diffractive multifocal focusing of radiation," *J. Quant. Electron.* **31**, 339–342 (2001).
6. R.R. Letfullin, O.A. Zayakin, and T.F. George, "Theoretical and experimental investigations of the effect of diffractive multifocal focusing of radiation," *Appl. Opt.* **40**, 2138–2147 (2001).
7. R.R. Letfullin and T.F. George, "Diffractive multifocal focusing of Gaussian beams," *Fiber and Integrated Optics* **21**, 145–161 (2002).
8. J.W. Goodman, *Introduction to Fourier Optics*, 60, McGraw-Hill, New York (1968).
9. E. Lommel, "Theoretical and experimental investigations of diffraction phenomena at a circular aperture and obstacle," *Bayerisch. Akad. d. Wiss.* **15**, 233 (1884).
10. M.S. Soskin and M.V. Vasnetov, "Singular optics," in *Progress in Optics*, E. Wolf, Ed., **42**, 219–276, Elsevier, Amsterdam (2001).
11. J.F. Nye and M.V. Berry, "Dislocations in wave trains," *Proc. Roy. Soc. London A* **336**, 165–190 (1974).
12. M. Born and E. Wolf, *Principles of Optics*, 7th ed., Sect. 8.8, Cambridge Univ. Press, Cambridge (1999).

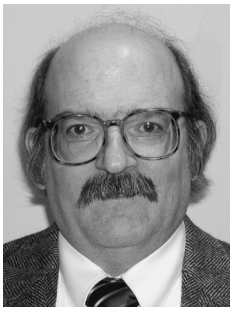

John T. Foley received his Ph.D. in Physics from the University of Rochester in 1978. His thesis advisor was Emil Wolf. He was post-doc at the University of Rochester for nine months, and then joined the faculty of Department of Physics and Astronomy at Mississippi State University, where he is currently Professor of Physics. He is the director of The Optics Project on the Web (WebTOP) an interactive, three-dimensional, computer graphics system for optics education. He is a Fellow of the Optical Society of America and received the 2003 George. P. Peagram Medal for excellence in teaching from the Southeastern Section of the American Physical Society.

Renat R. Letfullin earned his B.A. and M.S. in optics and spectroscopy from Samara State University (Russia) in 1984 and his Ph.D. in laser physics from Saratov State University in 1992. He is currently a Visiting Assistant Professor of Physics at Mississippi State University. Prior to 2002, he was a senior researcher in the Theoretical Department of the P.N. Lebedev Physical Institute of the Samara Branch of the Russian Academy of Sciences. He is known internationally as a theorist is in the fields of optics

and kinetics of chemical pulsed lasers, with special expertise on amplifiers in two-phase active media. Dr. Letfullin has published over 80 articles and conference proceedings, including three book chapters.

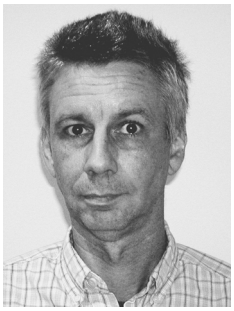

Henk F. Arnoldus obtained his Bachelor (1980) and Master (1981) degrees in Physics, both summa cum laude, from Eindhoven University of Technology, The Netherlands, with a specialization in heavy ion scattering theory. He then went to Utrecht University, The Netherlands, where he obtained his Ph.D. degree (1985) in Mathematics and Natural Sciences. From 1985 to 1988 he was postdoc with Thomas F. George in the Department of Physics at the University of New York at Buffalo. In 1988 he accepted a faculty position at Villanova University, Pennsylvania, where he stayed for six years. Currently, he is Associate Professor in the Department of Physics and Astronomy at Mississippi State University. He has published 84 papers and numerous conference proceedings, and he has edited three books. He has given 73 seminars/invited talks all over the world, including Russia, Denmark, and Korea.